J|A|C|S
ARTICLES
Published on Web 02/11/2006

Triradical Cation of *p*-Phenylenediamine Having Two Nitroxide Radical Groups: Spin Alignment Mediated by Delocalized Spin

Akihiro Ito,*,† Yoshiaki Nakano,† Masashi Urabe,† Tatsuhisa Kato,*,‡ and Kazuyoshi Tanaka*,†,§

Contribution from the Department of Molecular Engineering, Graduate School of Engineering, Kyoto University, Nishikyo-ku, Kyoto 615-8510, Japan, Department of Chemistry, Josai University, 1-1 Keyakidai, Sakado, Saitama 350-0295, Japan, and CREST, Japan Science and Technology Agency, Kawaguchi 332-0012, Japan

Received September 13, 2005; E-mail: aito@scl.kyoto-u.ac.jp; rik@josai.ac.jp; a51053@sakura.kudpc.kyoto-u.ac.jp

Abstract: The cationic state of a *p*-phenylenediamine (PDA) molecule having two nitroxide radical groups was prepared and characterized using electrochemical, electron spin resonance (ESR) spectroscopic, and absorption spectroscopic methods. The delocalized intervalence state of the *p*-phenylendiamine (PDA) moiety was detected in the cationic state. From the pulsed ESR measurements, it was confirmed that the delocalized spin induces parallel spin alignment between the localized two nitroxide groups which are magnetically weakly coupled in the neutral state. It was found that the resulting high-spin alignment does not seriously affect the delocalized intervalence state of the PDA radical cation.

Introduction

To control spin preference in multispin molecular systems, it should be established that a lot of stable organic radical centers are assembled to have desirable intramolecular magnetic interaction. In the past few decades, significant progress has been made in rational design and synthesis of high-spin organic molecules containing several stable radical centers.[1] In many cases, the stable radical centers are linked by the so-called ferromagnetic coupling units such as 1,3-benzenediyl to generate the (quasi-)degenerate singly occupied nonbonding molecular orbitals (NBMOs) according to Hund's rule.[2]

In addition, the control of charge distribution in the above-mentioned multispin organic molecular systems is also regarded as an important issue in conjunction with the potential application to spin electronics devices.[3] When a few electrons are added to or removed from the multispin organic system, important problems of the relationship between the spin preference and the extra charge distribution emerge from alterations to occupancy number of the NBMOs: whether the high-spin preference among the surviving unpaired electrons remains unchanged or not; whether the extra electrons (or "holes") are localized or delocalized.[2c] With these questions in mind, several polyradical anions[4] and cations[5] have exhibited intriguing aspects of the charge distribution and its influence on the spin preference.

Organic intervalence compounds are the simple models for understanding of the intramolecular electron-transfer process or for examining to what degree the extra charge is delocalized over a molecule, and nowadays a lot of delocalized intervalence compounds have been reported.[6−8] However, the delocalized spin associated with the delocalized intervalence state has never been used to mediate an intramolecular magnetic interaction, in particular, high-spin alignment. As has been described in our previous theoretical study,[3] the ferromagnetic coupling between the localized multispin system and the delocalized electron spin is closely related to the realization of spin-polarized molecular wire. In the present study, we report on the observation of spin alignment mediated by a delocalized spin in a multispin organic system. We selected *para*-phenylenediamine (PDA) derivative **1** carrying two persistent nitroxide groups (Figure 1) since radical cations of PDA molecules are widely accepted as important organic delocalized intervalence radical cations.[6,8] Furthermore, the relationship between spin alignment and intervalence state in $\mathbf{1}^+$ is also discussed in comparison with

† Kyoto University.
‡ Josai University.
§ Japan Science and Technology Agency.

(1) Crayston, J. A.; Devine, J. N.; Walton, J. C. *Tetrahedron* **2000**, *56*, 7829.
(2) (a) Dougherty, D. A. *Acc. Chem. Res.* **1991**, *24*, 88. (b) Iwamura, H.; Koga, N. *Acc. Chem. Res.* **1993**, *26*, 346. (c) Rajca, A. *Chem. Rev.* **1994**, *94*, 871.
(3) Ito, A.; Urabe, M.; Tanaka, K. *Polyhedron* **2003**, *22*, 1829 and references therin.
(4) (a) Matsushita, M.; Nakamura, T.; Momose, T.; Shida, T.; Teki, Y.; Takui, T.; Kinoshita, T.; Itoh, K. *J. Am. Chem. Soc*. **1992**, *114*, 7470. (b) Rajca, S.; Rajca, A. *J. Am. Chem. Soc*. **1995**, *117*, 9172. (c) Nakamura, T.; Momose, T.; Shida, T.; Kinoshita, T.; Takui, T.; Teki, Y.; Itoh, K. *J. Am. Chem. Soc*. **1995**, *117*, 11292. (d) Nakamura, T.; Momose, T.; Shida, T.; Sato, K.; Nakazawa, S.; Kinoshita, T.; Takui, T.; Itoh, K.; Okuno, T.; Izuoka, A.; Sugawara, T. *J. Am. Chem. Soc*. **1996**, *118*, 8684. (e) Sedó, J.; Ruiz, D.; Vidal-Gancedo, J.; Rovira, C.; Bonvoisin, J.; Launay, J.-P.; Veciana, J. *Adv. Mater*. **1996**, *8*, 748.
(5) (a) Matsushita, M.; Nakamura, T.; Momose, T.; Shida, T.; Teki, Y.; Takui, T.; Kinoshita, T.; Itoh, K. *Bull. Chem. Soc. Jpn*. **1993**, 66, 1333. (b) Izuoka, A.; Hiraishi, M.; Abe, T.; Sugawara, T.; Sato, K.; Takui, T. *J. Am. Chem. Soc*. **2000**, *122*, 3234. (c) Nakazaki, J.; Chung, I.; Matsushita, M. M.; Sugawara, T.; Watanabe, R.; Izuoka, A.; Kawada, Y. *J. Mater. Chem*. **2003**, *13*, 1011. (d) Harada, G.; Jin, T.; Izuoka, A.; Matsushita, M. M.; Sugawara, T. *Tetrahedron Lett*. **2003**, *44*, 4415.
(6) (a) Nelsen, S. F. *Chem.—Eur. J*. **2000**, *6*, 581. (b) Launay, L.-P. *Chem. Soc. Rev*. **2001**, *30*, 386.

 10.1021/ja056318e CCC: $33.50

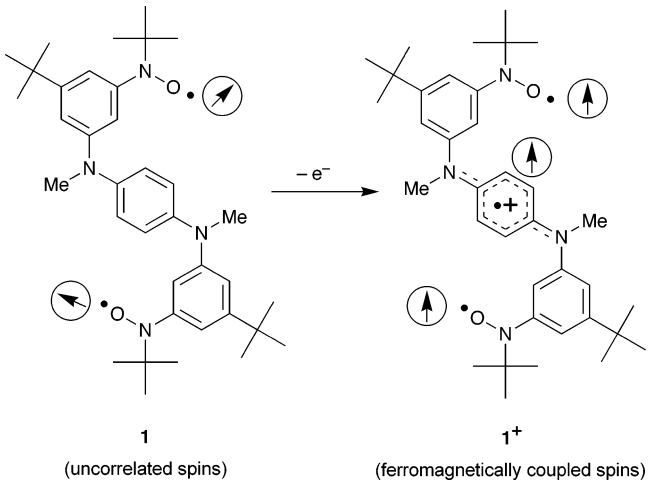

Figure 1. Spin alignment mediated by intervalence state in $\mathbf{1}^+$.

the intervalence compound, *N*,*N*′-dimethyl-*N*,*N*′-diphenyl-*p*-phenylenediamine (**3**) radical cation.

Experimental Section

^{1}H and ^{13}C spectra were recorded on a JEOL JNM-AL400 or a JNM-EX400 spectrometer, and chemical shifts are given in parts per million (ppm) relative to internal tetramethylsilane (δ 0.00 ppm). Elemental analyses were performed by the Center for Organic Elemental Microanalysis, Kyoto University.

Toluene and *n*-butyronitrile were distilled from CaH_2 under an argon atmosphere, tetrahydrofuran (THF) was distilled from sodium benzophenone or potassium benzophenone under an argon atmosphere, *N*,*N*-dimethylformamide (DMF) was dried over molecular sieves 4A, and benzonitrile was purified through an alumina (ICN, Alumina N, Akt. I) column with bubbling of argon, just before use. All the other purchased reagents and solvents were used without further purification. Column chromatography was performed using silica gel (Kanto Chemical Co., Inc., Silica gel 60N, spherical neutral) or alumina (Kanto Chemical Co., Inc., Aluminum Oxide, Activated for column chromatography).

***N*,*N*′-Bis[3-*tert*-butyl-5-(*N*-(*tert*-butyldimethylsiloxy)-*N*-*tert*-butylamino)phenyl]-*N*,*N*′-dimethyl-*p*-phenylenediamine (7).** A mixture of **5** (1.50 g, 11.0 mmol), *N*-(3-bromo-5-*tert*-butylphenyl)-*N*-(*tert*-butyldimethylsiloxy)-*N*-*tert*-butylamine (**6**)[9] (10.0 g, 24.1 mmol), NaO*t*Bu (2.50 g, 25.5 mmol), $Pd(OAc)_2$ (150 mg, 0.65 mmol), and 2-(di-*tert*-butylphosphino)biphenyl (150 mg, 0.50 mmol) in toluene was refluxed for 1 day. The resulting mixture was concentrated by evaporation under reduced pressure. The residue was diluted with Et_2O and water, and the resulting organic layer was separated and dried over $MgSO_4$. After evaporation of the solvent, the crude product was chromatographed on silica gel (CH_2Cl_2/*n*-hexane = 1:4 as eluent) to afford **7** (4.80 g, 54%) as a white solid: ^{1}H NMR (400 MHz, C_6D_6) δ 6.96−6.99 (m, 8H), 6.91 (br-s, 2H), 3.07 (s, 6H), 1.30 (s, 18H), 1.21 (s, 18H), 1.03 (s, 18H), 0.93 (br-s, 12H); ^{13}C NMR (100 MHz, C_6D_6) δ 151.9, 151.0, 148.8, 144.3, 122.7, 115.6, 114.5, 113.6, 61.0, 40.6, 35.0, 31.6, 26.6, 26.5, 18.4, −4.2. Anal. Calcd for $C_{48}H_{82}N_4O_2Si_2$: C, 71.76; H, 10.29; N, 6.97. Found: C, 71.58; H, 10.44; N, 6.81.

***N*,*N*′-Bis[3-*tert*-butyl-5-(*N*-*tert*-butyl-*N*-hydroxyamino)phenyl]-*N*,*N*′-dimethyl-*p*-phenylenediamine (8).** To an ice-cooled solution of **7** (564 mg, 0.70 mmol) in 5 mL of THF were added slowly 7 mL (7 mmol) of a 1.0 M solution of tetrabutylammonium fluoride in THF. Stirring was continued for 45 min at 0 °C and for 2 h at room temperature. After addition of water and Et_2O, the organic layer was separated, and the aqueous layer was extracted with Et_2O. The organic layers were combined and dried over $MgSO_4$. By evaporation under reduced pressure, a slightly reddish brown solid was obtained and washed with *n*-hexane containing a small amount of Et_2O to give **8** (355.4 mg, 88%) as a white solid: ^{1}H NMR (400 MHz, acetone-d_6) δ 7.36 (br-s, 2H), 6.96 (s, 4H), 6.84 (t, J = 1.9 Hz, 2H), 6.79 (t, J = 1.9 Hz, 2H), 6.73 (t, J = 1.9 Hz, 2H), 3.27 (s, 6H), 1.26 (s, 18H), 1.11 (s, 18H); ^{13}C NMR (100 MHz, acetone-d_6) δ 151.8, 151.0, 149.2, 144.4, 122.6, 115.4, 114.0, 113.3, 60.3, 40.8, 35.2, 31.6, 26.6.

***N*,*N*′-Bis[3-*tert*-butyl-5-(*N*-*tert*-butyl-*N*-oxylamino)phenyl]-*N*,*N*′-dimethyl-*p*-phenylenediamine (1).** To a solution of **8** (76 mg, 0.13 mmol) in CH_2Cl_2 (10 mL) was added an excess of Ag_2O (308 mg, 1.3 mmol), and the mixture was stirred for 2 h. After filtration through Celite, the solvent was evaporated under reduced pressure. The residue was chromatographed on silica gel (Et_2O/CH_2Cl_2/*n*-hexane = 1:4:5 as eluent) to afford **1** (63 mg, 83%) as a red solid: ESR (toluene at room temperature) g = 2.006, $|a_N|$ = 6.3 G; FAB HRMS (*m*-nitrobenzyl alcohol) *m*/*z* (relative intensity %) calcd for $C_{36}H_{52}N_4O_2$ $[M]^+$ 572.4090, found 572.4085 (7.4); $C_{36}H_{53}N_4O_2$ $[M + H]^+$ 573.4169, found 573.4162 (6.2); $C_{36}H_{54}N_4O_2$ $[M + 2H]^+$ 574.4247, found 574.4208 (7.4). Anal. Calcd for $C_{36}H_{52}N_4O_2$: C, 75.48; H, 9.15; N, 9.78; O, 5.59. Found: C, 75.36; H, 9.10; N, 9.60; O, 5.58.

Electrochemical Measurements. The cyclic voltammetry (CV) measurements were carried out in benzonitrile solution containing 0.1 M *n*-tetrabutylammonium tetrafluoroborate (*n*-Bu_4NBF_4) as a supporting electrolyte (25 °C, scan rate 100 mV/s) using an ALS/chi Electrochemical Analyzer model 612A. A three-electrode assembly was used, which was equipped with a platinum disk (2 mm^2), a platinum wire, and Ag/0.01 M $AgNO_3$ (acetonitrile) as the working electrode, the counter electrode, and the reference electrode, respectively. The redox potentials were referenced against a ferrocene/ferrocenium (Fc/Fc^+) couple.

UV/vis/NIR Spectrum Measurements. UV/vis/NIR spectra were obtained with a Perkin-Elmer Lambda 19 spectrometer. Spectroelectrochemical measurements were carried out with a custom-made optically transparent thin-layer electrochemical (OTTLE) cell (light pass length = 1 mm) equipped with a platinum mesh, a platinum coil, and a silver wire as the working electrode, the counter electrode, and the pseudo-reference electrode, respectively. The potential was applied with an ALS/chi Electrochemical Analyzer model 612A.

ESR Measurements. ESR spectra were recorded on a JEOL JES-SRE2X or a JEOL JES-TE200 X-band spectrometer, in which the temperature was controlled by a JEOL DVT2 variable-temperature unit or an Oxford ITC503 temperature controller combined with an ESR 910 continuous flow cryostat, respectively. A Mn^{2+}/MnO solid solution was used as a reference for the determination of *g*-values and hyperfine coupling constants. Pulsed ESR measurements were carried out on a Bruker ELEXES E580 X-band FT ESR spectrometer.

(7) (a) Mazur, S.; Schroeder, A. H. *J. Am. Chem. Soc*. **1978**, *100*, 7339. (b) Nelsen, S. F.; Thomson-Colon, J. A.; Katfory, M. *J. Am. Chem. Soc*. **1989**, *111*, 2809. (c) Almlöf, J. E.; Feyereisen, M. W.; Josefiak, T. H.; Miller, L. L. *J. Am. Chem. Soc*. **1990**, *112*, 1206. (d) Maslak, P.; Augustine, M. P.; Burkey, J. D. *J. Am. Chem. Soc*. **1990**, *112*, 5359. (e) Utamapanya, S.; Rajca, A. *J. Am. Chem. Soc*. **1991**, *113*, 9242. (f) Telo, J. P.; Shohoji, M. C. B. L.; Herold, B. J.; Grampp, G. *J. Chem. Soc., Faraday Trans*. **1992**, *88*, 47. (g) Bonvoisin, J.; Launay, J.-P.; Van der Auweraer, M.; De Schryver, F. C. *J. Phys. Chem*. **1994**, *98*, 5052. (h) Lahil, K.; Moradpour, A.; Bowlas, C.; Menou, F.; Cassoux, P.; Bonvoisin, J.; Launay, J.-P.; Dive, G.; Dehareng, D. *J. Am. Chem. Soc*. **1995**, *117*, 9995. (i) Bonboisin, J.; Launay, J.-P.; Verbouwe, W.; Van der Auweraer, M.; De Schryver, F. C. *J. Phys. Chem*. **1996**, *100*, 17079. (j) Nelsen, S. F.; Tran, H. Q.; Nagy, M. A. *J. Am. Chem. Soc*. **1998**, *120*, 298. (k) Lambert, C.; Gaschler, W.; Schmälzlin, E.; Meerholz, K.; Bräuchle, C. *J. Chem. Soc., Perkin Trans 2* **1999**, 577. (l) Rovira, C.; Ruiz-Molina, D.; Elsner, O.; Vidal-Gancedo, J.; Bonvoisin, J.; Launay, J.-P.; Veciana, J. *Chem.—Eur. J*. **2001**, *7*, 240. (m) Mayor, M.; Büschel, M.; Fromm, K. M.; Lehn, J.-M.; Daub, J. *Chem.—Eur. J*. **2001**, *7*, 1266. (n) Lambert, C.; Nöll, G.; Hampel, F. *J. Phys. Chem. A* **2001**, *105*, 7751. (o) Lindeman, S. V.; Rosokha, S. V.; Sun, D.; Kochi, J. K. *J. Am. Chem. Soc*. **2002**, *124*, 842. (p) Lambert, C.; Nöll, G. *Chem.—Eur. J*. **2002**, *8*, 3467. (q) Dumur, F.; Gautier, N.; Gallego-Planas, N.; Sahin, Y.; Levillain, E.; Masino, M.; Girlando, A.; Lloveras, V.; Vidal-Gancedo, J.; Veciana, J.; Rovira, C. *J. Org. Chem*. **2004**, *69*, 2164.
(8) (a) Lambert, C.; Nöll, G. *J. Am. Chem. Soc*. **1999**, *121*, 8434. (b) Lambert, C.; Nöll, G.; Schelter, J. *Nat. Mater*. **2002**, *1*, 69. (c) Lambert, C.; Nöll, G. *J. Chem. Soc., Perkin Trans. 2* **2002**, 2039.
(9) Ishida, T.; Iwamura, H. *J. Am. Chem. Soc*. **1991**, *113*, 4238.

Scheme 1

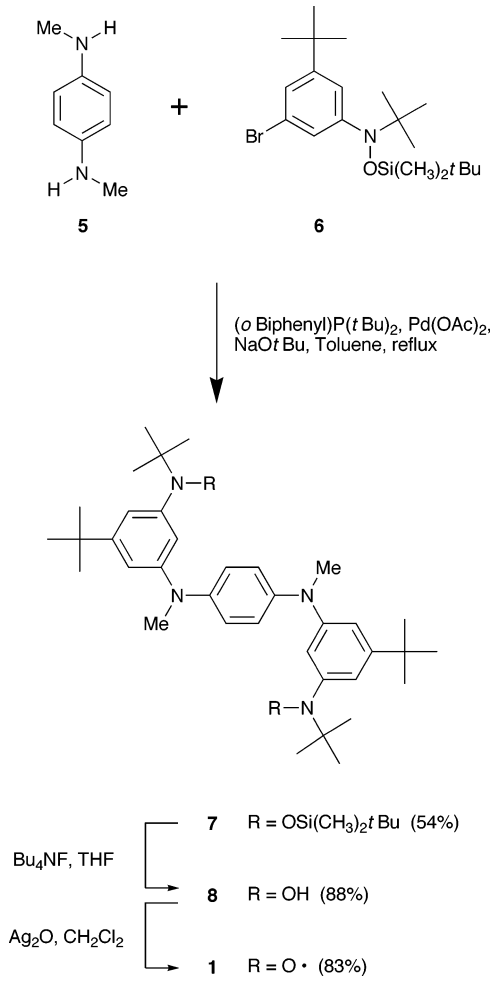

Magnetic Susceptibility Measurements. Magnetic susceptibilities of the powder samples were measured by a Quantum Design MPMS-5S system. The raw data were corrected for both the magnetization of the sample holder alone and the diamagnetic contribution of the sample itself. The estimation of the diamagnetic contribution was done by using Pascal's constants.

Results and Discussion

As shown in Scheme 1, the bisnitroxide **1** was prepared in three steps. The coupling reaction of *N*,*N*′-dimethyl-*p*-phenylenediamine **5** with the protected hydroxylamine **6** in the presence of palladium catalyst affords the precursor **7**. After desilylation of **7** with tetrabutylammonium fluoride, the desired bisnitroxide **1** was obtained as a reddish brown solid by oxidation of the bishydroxylamine **8** with Ag_2O.

A prerequisite for generating a triradical cation of **1** is that the central PDA moiety has a lower oxidation potential than those of the two nitroxide groups. The oxidation potentials of **1** were evaluated by cyclic voltammetry in a benzonitrile solution at 298 K. The observed voltammogram showed three oxidation waves (Figure 2b). The first oxidation process was found to be reversible by lowering the turnaround potential (Figure 2a). From the comparison of the oxidation potentials for **3** with that for the *tert*-butylphenyl nitroxide (**4**)(Scheme 2), the first reversible oxidation wave of **1** can be ascribed to the removal of one electron from the central PDA moiety (Table 1). The remaining two oxidation peaks probably correspond to

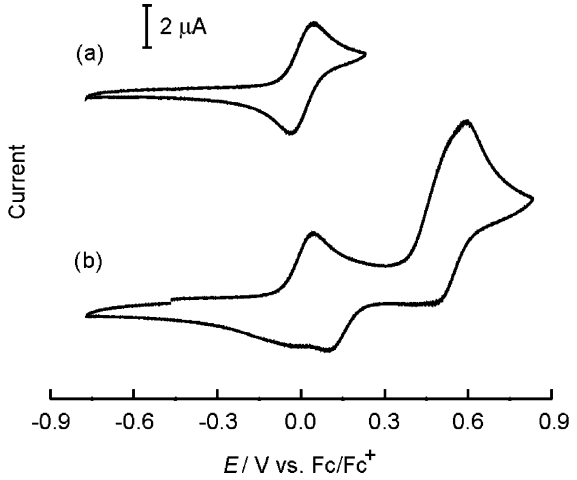

Figure 2. Cyclic voltammograms of **1** in PhCN containing 0.1 M *n*-Bu_4NBF_4 at 298 K (scan rate 0.1 V s^{-1}): (a) the scan at lower turnaround potential and (b) the scan at higher turnaround potential.

Scheme 2

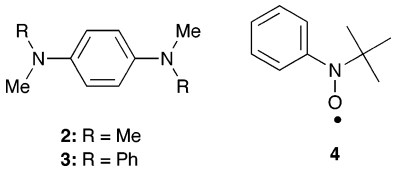

Table 1. Redox Potentials (V) of **1** and Related Compounds[a]

compd	E_1	E_2	E_3
1	0.00	0.52[b]	0.55
3	−0.02	0.48	
4	0.41[b]		

[a] 0.1 M *n*-Bu_4NBF_4 in PhCN, potential versus Fc/Fc^+, Pt electrode, 298 K, scan rate 100 mV/s. [b] Oxidation peak potential.

the oxidation process of the nitroxide groups and/or the oxidation process from a semiquinone to quinone of the central PDA moiety. It is interesting to note that the difference between the first and second oxidation potentials of PDA derivatives (ΔE) is closely related to the twist angle between the amino group and 1,4-phenylenediyl, which determines the electronic coupling between charge-bearing units.[10] Although the rigorous value of ΔE for **1** is not obtained owing to the overlap of the second and third oxidation processes, the ΔE can be roughly estimated to be 0.52−0.55 V, similar to the value 0.5 V for **3**. This suggests that the substituting nitroxide groups do not seriously affect the twist angle between the amino group and 1,4-phenylenediyl.

The observed continuous wave ESR (cw-ESR) spectrum of **1** in a frozen *n*-butyronitrile solution consisted of a single signal with unresolved hyperfine and/or fine structure at 123 K. In addition, the forbidden $\Delta M_S = \pm 2$ resonance was also observed, suggesting the presence of the triplet state between the two nitroxide groups in **1**. On the other hand, the temperature dependence of the magnetic susceptibility measured by a SQUID magnetometer exhibited a very weak ferromagnetic interaction between the two nitroxide groups in **1** ($J/k_B = 0.6$ K).[11] This

(10) Nishiumi, T.; Nomura, Y.; Chimoto, Y.; Higuchi, M.; Yamamoto, K. *J. Phys. Chem. B* **2004**, *108*, 7992.
(11) The temperature dependence of magnetic susceptibility for **1** was analyzed by the modified Bleaney−Bowers equation for singlet−triplet model. Bleaney, B.; Bowers, K. D. *Proc. R. Soc., London Ser. A* **1952**, *214*, 451.

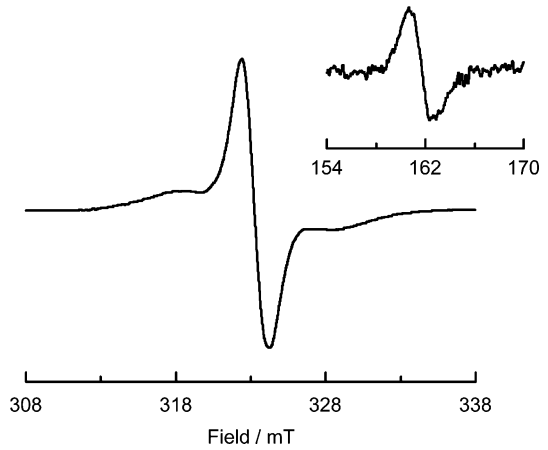

Figure 3. cw-ESR spectrum of $\mathbf{1}^+$ in *n*-butyronitrile at 123 K. Inset: The forbidden $\Delta M_S = \pm 2$ resonance at 123 K.

indicates that the two nitroxide groups are virtually magnetically uncoupled. On the other hand, in the cw-ESR spectrum of the oxidized species of **1** treated with up to 1 molar equiv of tris-(4-bromophenyl)aminium hexachloroantimonate at 195 K, no definite fine-structured spectrum characteristic of the spin quartet state was observed at 123 K, although broad shoulders were seen beside the intense central line (Figure 3). However, the half-field resonance corresponding to the $\Delta M_S = \pm 2$ transition was detected, and furthermore, the signal intensity of this forbidden transition was inversely proportional to temperature, suggesting the possibility of a high-spin ground state of the triradical cation $\mathbf{1}^+$. In addition, the DFT calculations (UB3LYP/6-31G*) on the cation of the simplified model compound for **1** gave the energy difference between the doublet and quartet states (ΔE_{D-Q}) of 0.81 kcal/mol, supporting the spin quartet ground state for the triradical cation $\mathbf{1}^+$.[12] To identify unequivocally spin multiplicity of the triradical cation $\mathbf{1}^+$ at low temperature, we measured the electron spin transient nutation (ESTN) spectrum based on the pulsed ESR method (Figure 4).[13] Judging from the ratio[13] between the nutation frequency in question and that for the $|S, M_S\rangle = |^1/_2, +^1/_2\rangle \leftrightarrow |^1/_2, -^1/_2\rangle$ transition (23 MHz), the main nutation signals observed at 39 and 45 MHz were found to be assignable to $|S, M_S\rangle = |^3/_2, \pm^3/_2\rangle \leftrightarrow |^3/_2, \pm^1/_2\rangle$ and $|^3/_2, {}^1/_2\rangle \leftrightarrow |^3/_2, -^1/_2\rangle$ transitions, respectively. The weak nutation signal at 33 MHz corresponds to the $|1, 0\rangle \leftrightarrow |1, \pm 1\rangle$ transition of neutral **1**. This also supports that the spin quartet state of $\mathbf{1}^+$ is dominant at 5 K.

To confirm the presence of the intervalence state in triradical cation $\mathbf{1}^+$, the best way is to observe the characteristic lowest-

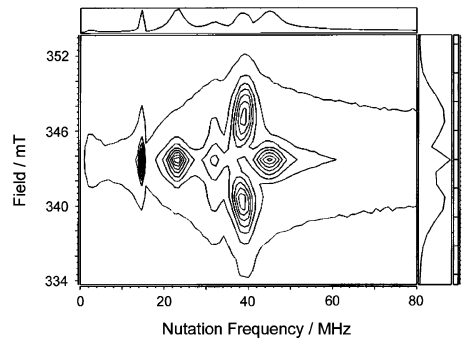

Figure 4. ESTN spectrum of $\mathbf{1}^+$ in frozen *n*-butyronitrile solution at 5 K [**1** was oxidized with tris(4-bromophenyl)aminium hexachloroantimonate].

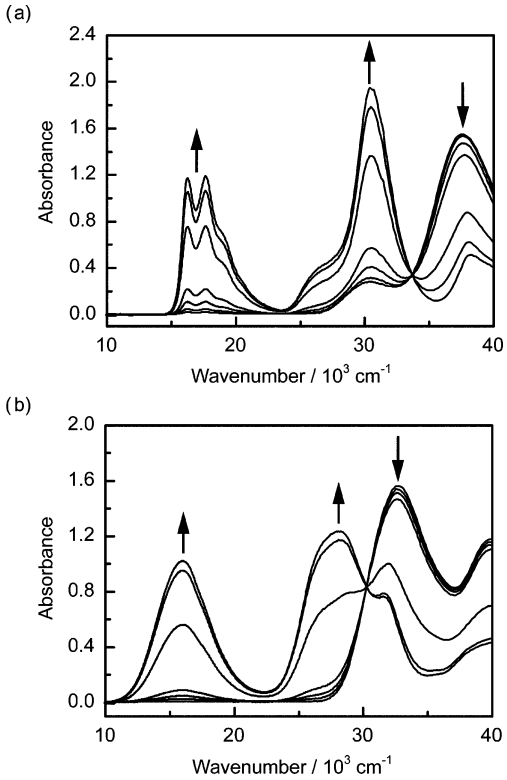

Figure 5. Spectroelectrochemical study of (a) **2** to $\mathbf{2}^+$ and (b) **3** to $\mathbf{3}^+$ in CH_2Cl_2/0.1 M *n*-Bu_4NBF_4 at room temperature.

energy absorption band. According to Robin and Day,[14] the intervalence compounds are classified into three categories on the basis of the size of the electronic interaction (H) between the charge-bearing units: Class I compounds have complete charge localization ($H = 0$), Class II compounds have intermediate electronic interaction that allows partial charge delocalization between two charge-bearing units, and in Class III compounds, the electronic interaction is so strong that the charge is fully delocalized over two charge-bearing units. In Class II compounds, the lowest-energy absorption band (intervalence band) has a very broad Gaussian-shaped peak that is explainable by charge transfer between two charge-bearing units, as pointed out by Hush.[15] On the other hand, delocalized Class III compounds exhibit rather narrow intervalence bands with a partially resolved vibrational fine structure.[16,17] Therefore, we

(12) For the neutral and cationic state of **1** and **3**, the hybrid HF/DF (B3LYP) calculations were performed by using 6-31G* basis sets. For **1**, all *tert*-butyl groups were replaced by the methyl groups. Full geometry optimizations were carried out under C_i symmetrical constraint. All the calculations were done with the Gaussian 98 program package.

(13) The magnetic moments with distinct spin quantum numbers (S) precess with their specific nutation frequency (ω_n) in the presence of a microwave irradiation field and a static magnetic field. The nutation frequency for a transition from $|S, M_S\rangle$ to $|S, M_S + 1\rangle$ can be expressed as $\omega_n = [S(S+1) - M_S(M_S+1)]^{1/2}\omega_0$ under certain conditions. This indicates that ω_n can be scaled with the total spin quantum number S and the spin magnetic quantum number M_S in the unit ω_n ($=\omega_0$) for the doublet species; $\sqrt{2}$ for $S = 1$, $\sqrt{3}$ and 2 for $S = {}^3/_2$. For determination of spin multiplicity for high-spin molecules by using the pulsed ESR technique, see: (a) Isoya, J.; Kanda, H.; Norris, J. R.; Tang, J.; Brown, M. K. *Phys. Rev. B* **1990**, *41*, 3905. (b) Astashkin, A. V.; Schweiger, A. *Chem. Phys. Lett.* **1990**, *174*, 595. (c) Sato, K.; Yano, M.; Furuichi, M.; Shiomi, D.; Takui, T.; Abe, K.; Itoh, K.; Higuchi, A.; Katsuma, K.; Shirota, Y. *J. Am. Chem. Soc.* **1997**, *119*, 6607. (d) Ito, A.; Ino, H.; Matsui, Y.; Hirao, Y.; Tanaka, K.; Kanemoto, K.; Kato, T. *J. Phys. Chem. A* **2004**, *108*, 5715.

(14) Robin, M.; Day, P. *Adv. Inorg. Chem. Radiochem.* **1967**, *10*, 247.

(15) (a) Hush, N. S. *Prog. Inorg. Chem.* **1967**, *8*, 391. (b) Hush, N. S. *Electrochem. Acta* **1968**, *13*, 1005. (c) Creutz, C. *Prog. Inorg. Chem.* **1983**, *30*, 1. (d) Hush, N. S. *Coord. Chem. Rev.* **1985**, *64*, 135.

(16) Bailey, S. E.; Zink, J. I.; Nelsen, S. F. *J. Am. Chem. Soc.* **2003**, *125*, 5939.

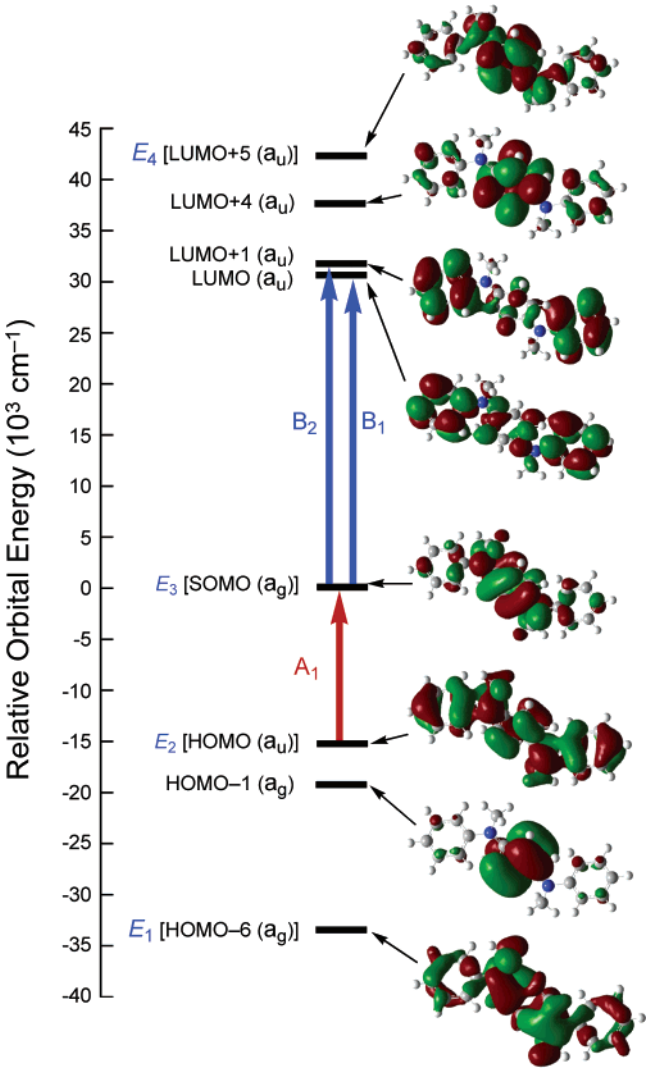

Figure 6. Lower-energy NCG transitions (Hoijtink type A and B transitions) and the selected frontier MO levels for $\mathbf{3}^+$ at the B3LYP/6-31G* level. The E_1 to E_4 MO levels are derived from partial orbital interaction between the diabatic orbitals of two charge-bearing units and the benzene e_{1g} HOMOs and e_{2u} LUMOs. HOMO-1 (and LUMO+4) stems from the remaining benzene e_{1g} HOMO (and e_{2u} LUMO).

have measured the UV/vis/NIR absorption spectral change during the course of the oxidation of **1** by using an optically transparent thin-layer electrochemical cell. For a reference, the spectral changes of *N*,*N*,*N*′,*N*′-tetramethyl-*p*-phenylenediamine (**2**) and *N*,*N*′-dimethyl-*N*,*N*′-diphenyl-*p*-phenylenediamine (**3**) were also measured in the same experimental condition.

As shown in Figure 5a, the two absorption bands E_A and E_B, which correspond to the lowest- and next-lowest-energy bands, respectively, grew upon oxidation of **2** to the monoradical cation $\mathbf{2}^+$, and the lowest-energy band (E_A) showed a typical vibrational fine structure, as examined by Nelsen et al.[16] On the other hand, the E_A band in $\mathbf{3}^+$ was a broad one with an unresolved vibrational fine structure (Figure 5b). This broad E_A band in $\mathbf{3}^+$ is also seen in some *N*,*N*,*N*′,*N*′-tetraaryl-*p*-phenylenediamine radical cations. Recently, the detailed study on the *N*,*N*,*N*′,*N*′-tetraphenyl-*p*-phenylenediamine radical cation concluded that the radical cation adopts a delocalized Class III structure both

Table 2. Observed and Koopmans-Based Transition Energies for *p*-Phenylenediamine Intervalence Radical Cations in CH_2Cl_2

compd	E_A (obsd) (cm^{-1})	A_1 (cm^{-1})	E_B (obsd) (cm^{-1})	B_1 (and B_2) (cm^{-1})
1	14 430	15 210[a]	25 510	29 810[a] (33 810[a])
2	16 260	18 330[b]	26 390 (sh) 30 400	29 710[b] (33 310[b])
3	15 950	15 790[c]	26 530 (sh) 28 250	30 900[c] (31 220[c])

[a] UB3LYP/6-31G* calcd. [b] B3LYP/6-31G* calcd from ref 20. [c] B3LYP/6-31G* calcd.

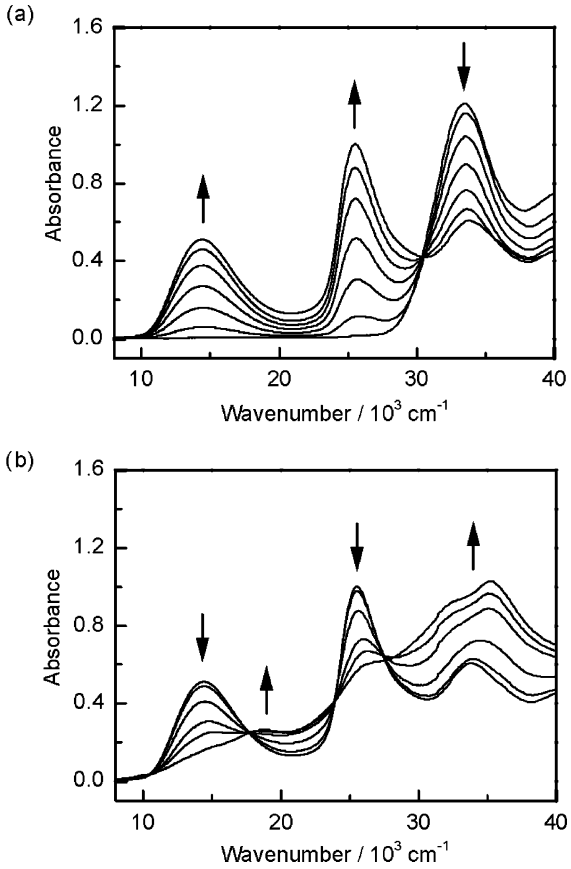

Figure 7. Spectroelectrochemical study of **1** in CH_2Cl_2/0.1 M *n*-Bu_4NBF_4 at room temperature: (a) **1** to $\mathbf{1}^+$ and (b) $\mathbf{1}^+$ to $\mathbf{1}^{2+}$.

in the solid state and in solution, despite the broad E_A band shape which was different from that of the delocalized Class III compound $\mathbf{1}^+$.[18] Moreover, Nelsen et al. pointed out that the Marcus−Hush two-state model should not be applicable to the delocalized Class III system and that the transition energy obtained from the E_A absorption band does not directly relate to the electronic interaction between two charge-bearing units.[19,20] Delocalized intervalence compounds have symmetrical charge distributions and, hence, have a charge on the bridging *p*-phenylene moiety. As is apparent from Figure 6, the partial molecular orbital interaction between the diabatic orbitals originating from two charge-bearing units and the benzene e_{1g}

(17) Nelsen, S. F.; Konradsson, A. E.; Weaver, M. N.; Telo, J. P. *J. Am. Chem. Soc.* **2003**, *125*, 12493.

(18) Szeghalmi, A. V.; Erdmann, M.; Engel, V.; Schmitt, M.; Amthor, S.; Kriegisch, V.; Nöll, G.; Stahl, R.; Lambert, C.; Leusser, D.; Stalke, D.; Zabel, M.; Popp, J. *J. Am. Chem. Soc.* **2004**, *126*, 7834.

(19) Nelsen, S. F.; Weaver, M. N.; Zink, J. I.; Telo, J. P. *J. Am. Chem. Soc.* **2005**, *127*, 10611.

(20) Nelsen, S. F.; Weaver, M. N.; Telo, J. P.; Lucht, B. L.; Barlow, S. *J. Org. Chem.* **2005**, *70*, 9326.

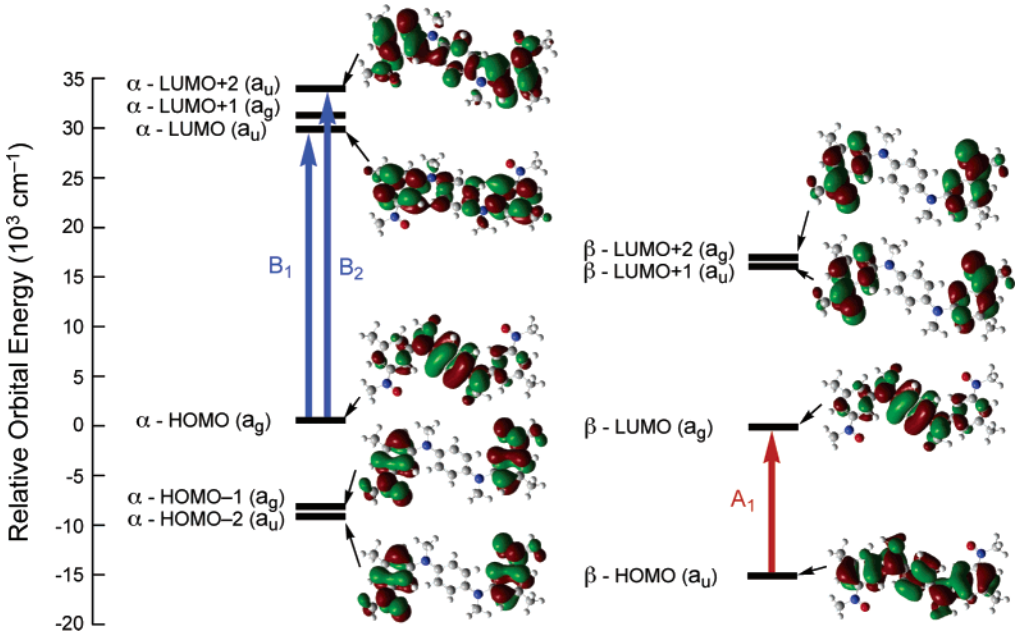

Figure 8. Lower NCG transition energies (Hoijtink type A and B transitions) and the selected frontier MO levels for model compounds of $\mathbf{1}^+$ at the UB3LYP/6-31G* level. The transition from α(HOMO) to α(LUMO+1) is forbidden.

HOMOs and e_{2u} LUMOs leads to four adiabatic MOs, shown as E_1 to E_4 (neighboring orbital model[19]).[12] In this situation, the lowest transition energy in the optical spectra corresponds to the promotion of an electron from the HOMO to the singly occupied MO (SOMO) (Hoijtink type A transition) or that from the SOMO to LUMO (Hoijtink type B transition).[21] These transition energies in delocalized intervalence compounds can be well estimated by single-point MO calculations with a neutral charge at optimized radical cation geometries (neutral in cation geometry or NCG)[19,20] on the basis of Koopmans' theorem. The observed transition energies and the Koopman-based band assignments by using the NCG method are summarized in Table 2. The calculated transition energies are in good agreement with the experimental values, and the E_A and E_B bands can be assigned to the Hoijtink type A and B transitions, respectively. Note that the E_B band of $\mathbf{3}^+$ has a shoulder. This is because the LUMO and LUMO+1 are quasi-degenerate (the calculated energy difference is 320 cm^{-1}) and have an a_u orbital symmetry (B_1 and B_2 transition in Figure 6). Such a shoulder peak is also observed in $\mathbf{2}^+$ (Figure 5a).

In the case of **1**, the E_A and E_B bands grew at 14 430 cm^{-1} and 25 510 cm^{-1}, respectively, upon oxidation to the monoradical cation $\mathbf{1}^+$, and further oxidation to the dication $\mathbf{1}^{2+}$ resulted in the disappearance of these two band, and a new band at 18 730 cm^{-1} was slightly apparent as shown in Figure 7. These spectral changes indicate that the delocalized electron spin was generated over the central PDA moiety after one-electron oxidation of **1**. Note that the same spectral changes were also seen by the chemical oxidation with $SbCl_5$ in CH_2Cl_2. For $\mathbf{1}^+$, the wave function obtained by the NCG calculation is of the unrestricted type (UB3LYP/6-31G*), and therefore, the MOs are actually split into α and β spin sets.[12] The lowest Hoijtink type A transition corresponds to one from β (HOMO) to β (LUMO), while the lowest Hoijtink type B transition corresponds to one from α (HOMO) to α (LUMO), as shown in Figure 8. From the comparison between Figures 6 and 8, the MOs associated with the type A and B transitions in $\mathbf{1}^+$ are similar to ones in $\mathbf{3}^+$, and furthermore, the MOs (α(HOMO-1) and α(HOMO-2)) originating from the nitroxide groups are well localized and are lower in energy than the MO (α(HOMO)) from the PDA radical cation. Therefore, it can be concluded that the two nitroxide groups do not greatly affect the delocalized intervalence band of the PDA moiety in $\mathbf{1}^+$.

In summary, we have demonstrated the first example of parallel spin alignment mediated by the delocalized intervalence state in a multispin organic molecule $\mathbf{1}^+$. The present triradical cation is also considered to be intriguing in that the localized and delocalized spins coexist in a single molecular system.

Acknowledgment. This work was supported by CREST (Core Research for Evolutional Science and Technology) of the Japan Science and Technology Agency (JST) and by a Grant-in-Aid for Scientific Research from the Japan Society for the Promotion of Science (JSPS). Thanks are due to the Research Center for Molecular-Scale Nanoscience, the Institute for Molecular Science for assistance in obtaining the pulsed ESR spectra.

JA056318E

(21) (a) Hoijtink, G. J.; Weijland, W. P. *Recl. Trav. Chim. Pays-Bas* **1957**, *76*, 836. (b) Buschow, K. J. J.; Dieleman, J.; Hoijtink, G. J. *Mol. Phys.* **1963**−**1964**, *7*, 1.